A New Inductive Proximity Sensor as a Guiding Tool for Removing Metal Shrapnel during Surgery

Mithun Sakthivel, Boby George, Jayashankar V. and Mohanasankar Sivaprakasam
Dept. of Electrical Engineering, Indian Institute of Technology Madras, Chennai, India
Email: msmithun83@gmail.com

***Abstract* – In this paper, an inductive proximity sensor with a longer range when compared to its diameter is presented. This sensor is intended to guide doctors, while performing surgery to remove metal shrapnel from victims of bomb blasts, gun fire, land mines etc. Presently doctors rely on imaging systems to locate shrapnel in the victim's body before surgery. Effectiveness of surgery and recovery solely depends on the doctors' skill to trace the shrapnel. In some cases the shrapnel may be visible in the images, but it may be untraceable during surgery. So in such cases, an inductive proximity sensor which is small enough to be introduced into the victim's body and can direct the recovery tool effectively to the exact location of the shrapnel, during the surgery, will be very useful to the doctor. Such a sensor, along with its details and experimental results are presented in this paper. This sensor works on a new comparison based method to detect tiny targets, as the detector size is a constraint here. The sensor can detect shrapnel materials such as steel, brass and Aluminium. A smaller, modified version of this sensor is also presented in the paper, along with a study of the effect of body tissues on sensor performance.**

Index terms – Shrapnel; metal detector; pulse induction; differential measurement; mutual induction; conductive targets; inductive targets.

I. INTRODUCTION

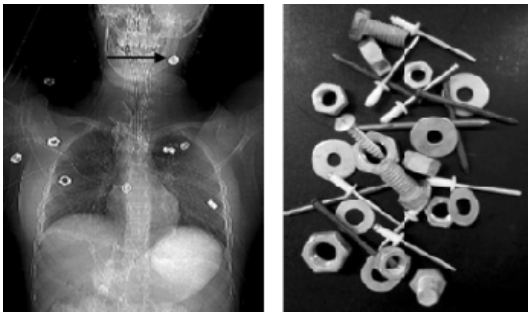

Fig. 1. CT image of shrapnel inside a bomb blast victim and typical metal objects used in a bomb [1].

One of the major causes of death in victims of bomb blasts, gun fire and mines is internal injury due to shrapnel. An X-ray image showing shrapnel inside the body of a blast victim and typical shrapnel materials observed in such incidents are shown in Fig. 1 [1]. Shrapnel are usually made of steel, copper and Aluminium [2], [3]. Presently, doctors rely on imaging systems like MRI or ultrasound or CT scan to locate the position of the shrapnel in the victim's body before surgery [4]. The recovery of the shrapnel is solely dependent on the doctors' skill to trace it during the surgery. In certain cases, the doctors can see the shrapnel clearly in the images, but the recovery may be extremely difficult if the shrapnel has penetrated deep into the tissues. This creates a clinical requirement for an online sensor that can be introduced into the body during the surgery to trace the shrapnel. Hence, an inductive proximity sensor which serves this purpose is proposed in this paper. Commercially available metal detectors are not suitable here, as their diameters should not be more than a few millimeters. Since the sensitivity of a metal detector is dependent on its cross sectional diameter, a new method is explained in this paper, to detect shrapnel even at depths greater than the diameter of the sensor. The experimental results from a prototype sensor developed, show that it can detect the presence of metal shrapnel accurately and can help the doctor to trace it easily by providing a suitable audio output.

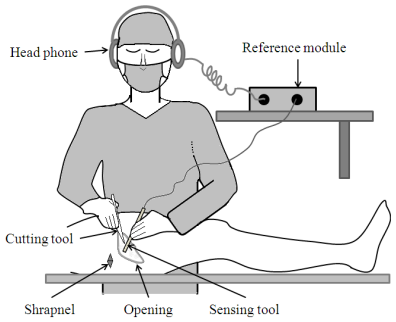

Fig. 2. Conceptual diagram of the sensor in application.

Fig. 2 shows a conceptual diagram of the mode of application. Here, the doctor first makes an opening near the area of penetration based on X-ray images and then introduces the sensor to trace it. The sensor provides feedback to the doctor as audio signals through the head phone. Based on the change in amplitude heard, the doctor moves the sensor further to trace the shrapnel and cuts further in the correct direction to reach the shrapnel.

II. NEW INDUCTIVE PROXIMITY SENSOR

The proposed Inductive Proximity Sensor (IPS) has an air-cored coil with a diameter of few millimeters (mm), as shown in Fig. 3. The coil can be excited by a Continuous Wave (CW) or Pulse Induction (PI) [6]. For the proposed sensor PI excitation is adopted, since a continuous high current is not recommended when the sensor is inserted into the body. The excitation field induces eddy currents in the metal target (shrapnel) and senses it by virtue of the changes in magnetic field associated with it [7]. The change in magnetic field can be sensed by measuring either the voltage across the sensor or

the current through it. In CW type, the eddy current in the target is produced by a continuous ac current. In PI type, a high dc current is applied to the coil which for a short duration. This induces a voltage in the coil whose rate of fall is determined by the metal target [6], [8].

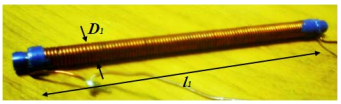

Fig. 3. Proposed inductive sensor; D_1 is the outer diameter of the sensor while l_1 is its total length.

The prototype sensor shown in Fig. 3 has number of turns n_1 = 104, length l_1 = 8 cm and diameter D_1 = 4.4 mm. Its measured inductance L_1 = 2.28 µH (with no shrapnel) and resistance R_1 = 400 mΩ. The above dimensions are small enough for inserting the sensing tool into the body, through an incision made near the area of penetration of the shrapnel. As mentioned before, the incision can be made after examining the X-ray image of the shrapnel from different angles that provide the shortest path to reach the shrapnel from the skin surface. Once introduced into the opening, the doctor can use the data from the sensor to determine the direction in which he/she has to cut further to reach the shrapnel.

The magnetic flux density B produced by a circular solenoid of n turns, radius r, length l and current I, at a distance z along its axis is given by (1),

$$B = \frac{\mu_0 \mu_r nI}{2l.}\left[\frac{(z+l)}{\sqrt{(r^2+(z+l)^2)}} - \frac{z}{\sqrt{(r^2+z^2)}}\right] \quad (1)$$

where μ_0 and μ_r are the permeability of free space and relative permeability of the medium respectively [9]. In equation (1), B falls exponentially with z. In general, metal detectors are sensitive up to a depth equal to their diameters [5]. But when the diameter is too small, as in this case, sensing shrapnel which have penetrated deep into the body will be very difficult using existing methods. Hence, a differential measurement approach is proposed here.

III. Differential Sensing

Conventional PI metal detectors use a single coil. But in this application, as the sensor diameter is very small, the change in its (coil) impedance due to the target cannot be distinguished with good accuracy. To improve the sensitivity, especially for greater depths, a secondary receiver coil is wound over the single coil (primary) shown in Fig. 3. When the primary coil is excited, due to mutual induction, secondary also gets some voltage induced. Amount of this induced voltage will be altered if a metal target is present in the vicinity of the coils. But this change in the induced voltage will be very small when compared to a vacant situation (no target), as the secondary coil is also small in diameter. Hence, measuring the change in output from a single primary-secondary pair may lead to erroneous tracking. In order to overcome this difficulty, an identical dummy unit (with primary B1 and secondary B2) was connected along with the sensor (with primary A1 and secondary A2) in a differential manner as indicated in Fig. 4. Magnetic characteristics of both the sensor and dummy are identical. Dummy is kept in the measurement unit as indicated in Fig. 4. Both the primary coils carry the same excitation current, but the sensor alone is exposed to the target (not the dummy). The receiver coils of the sensor and dummy are connected in a differential manner to obtain the change in output due to the target.

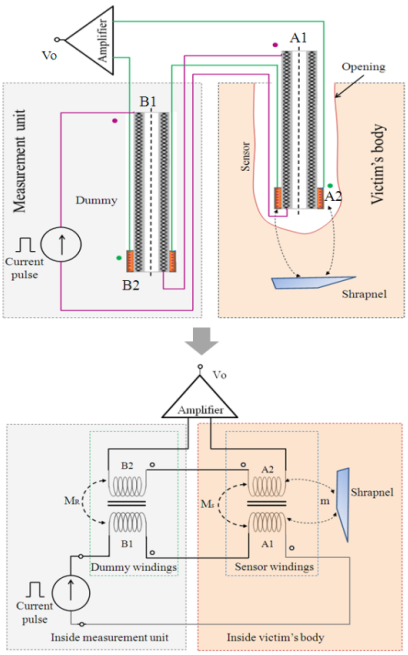

Fig. 4. Differential sensing scheme and simplified equivalent circuit.

As mentioned above, only the sensor (coils A1 and A2) is introduced into the victim's body, while the dummy (coils B1 and B2) is kept inside the measurement unit and acts as a reference. As in Fig. 4, the differential output from receiver coils is given to an amplifier whose output is a function of depth and properties of metal shrapnel in the body. A simplified equivalent circuit of the sensing scheme is also shown in Fig. 4.

A prototype circuit has been built. Its circuit diagram is shown in Fig. 5. Initially, output was recorded without any target (vacant) to evaluate how well the sensor and dummy are matched. The receiver windings (A2 and B2) had number of turns n_2 = 10, length l_2 = 7 mm and diameter D_2 = 5.8 mm with measured inductance L_2 = 430 nH and resistance of R_2 = 100 mΩ. The dc excitation was provided from a dc source and the current pulse was generated using a MOSFET whose gate was controlled by a voltage pulse from a function generator. The measurements were taken using an oscilloscope MSO6034A from Agilent Technologies. Full scale of the MSO was set to 200 mV. Fall time of the pulse was 10 µs. This is selected based on the frequency dependence of typical target materials [6]. Instrumentation amplifier INA129 with a gain of 62 was used to amplify the difference signal. It was noted that the two receiver outputs differed slightly even for a vacant condition. This was attributed to the differences in their geometrical construction. This produces a small offset voltage V_{OS} in the output. Now, when the sensor approaches the target, its output

will alone vary, producing a differential voltage V_d. Magnitude of V_d is indicative of presence and depth of the shrapnel.

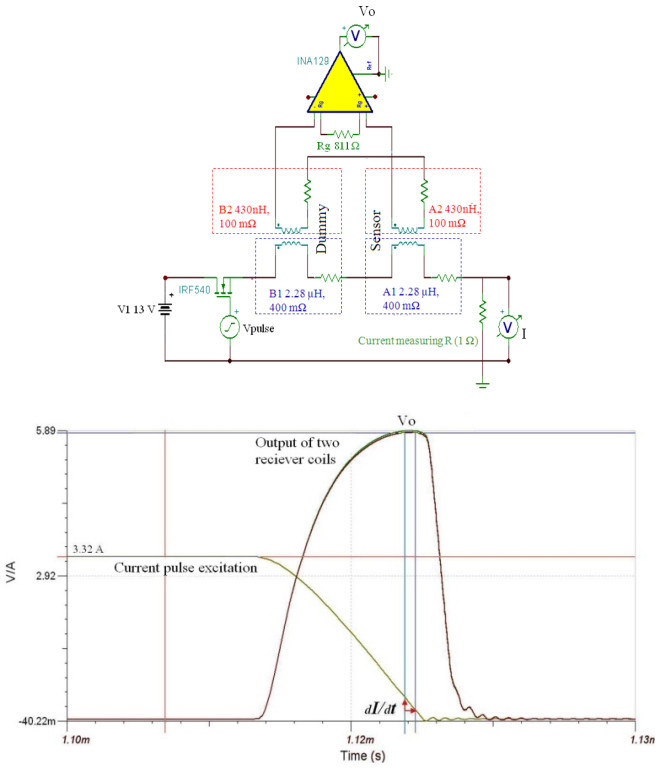

Fig. 5. Schematic of prototype circuit; the excitation current pulse along with the outputs of receiver coils of sensor and dummy are also shown. The two receiver coil outputs match well and hence any change in sensor output with respect to dummy can be easily obtained.

IV. Test Results

The shrapnel may be a conductive or an inductive target [10]. Various targets were placed along the axis of the sensor (in air) to evaluate the system performance.

A. Conductive target

Conductive targets are mostly paramagnetic and have low resistivity [10]. These are usually Aluminium (*Al*) or Copper alloys. For evaluation, an *Al* target of length 5 mm, 2.5 mm inner diameter (ID) and 5 mm outer diameter (OD) was used as the target. Output waveform obtained from the prototype for a pulse excitation is shown in Fig. 6a.

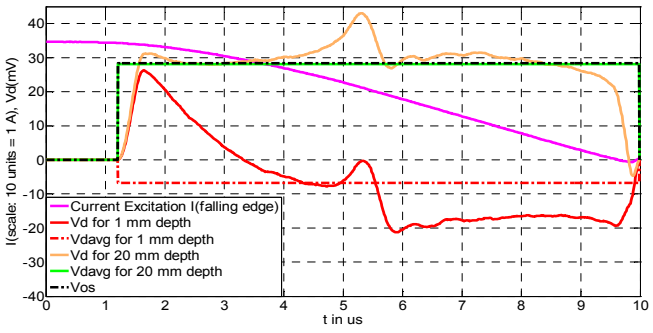

Fig. 6a. Excitation current and V_d of an *Al* target at various depths.

The average of signal V_d (V_{davg}) shown in Fig. 6a was computed during the excitation period and plotted against target depth in Fig. 6b. It was observed that, the V_{davg} decreased when the sensor was moved towards the target.

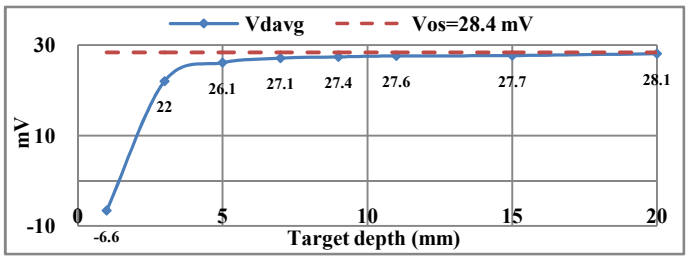

Fig. 6b. Average of V_d shown in Fig. 6a, computed and plotted against target depth. A threshold voltage V_T can be set close to *Vos* below which indicates the presence of the metal.

In the case of the conductive target, it acts as a resistive load as far as the sensor windings are concerned. The eddy current induced in the target produces a magnetic field that opposes the main exciting field. This reduces the voltage induced in the receiver winding (compared to the dummy receiver winding) due to which V_{davg} will also reduce. It can be seen that presence of *Al* target used in the experiment can be observed from a depth of about 20 mm.

B. Inductive target

Inductive targets are mostly ferromagnetic materials with reasonably large relative permeability compared to resistivity [10]. Steel is one such shrapnel material. Therefore a steel cylinder with length 5 mm, ID 2.5 mm and OD 6 mm was selected as target. Waveforms recorded from the MSO are shown in Fig. 7a. The V_{davg} for each depth are shown in Fig. 7b. For the selected target, V_{davg} seems to fall exponentially with depth and the maximum target depth detected was 25 mm.

In the case of an inductive target, signal induced in the receiver of the sensor increases, raising V_d, as the sensing head approaches the target. This can be represented as an equivalent increase in mutual inductance *m* between the primary and secondary of the sensor winding shown in Fig. 4. The increase in mutual inductance *m* can be computed approximately using (2) for each case shown in Fig. 7a. In (2), *dI/dt* is the rate of change of current during this period (= 280 mA/µs).

$$m = \left[\frac{V_{davg} - V_{os}}{dI/dt} \right] \qquad (2)$$

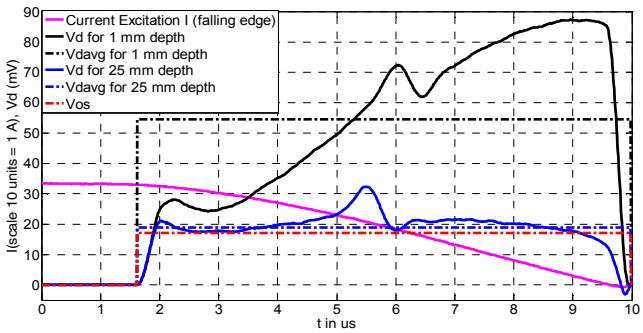

Fig. 7a. Excitation current and V_d of a steel target for various depths.

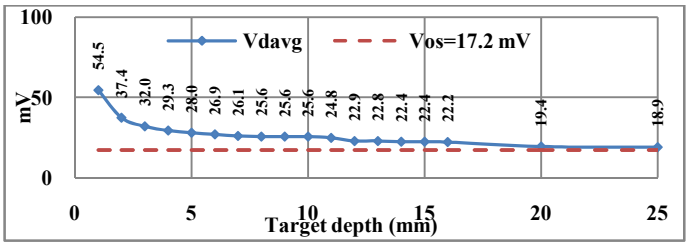

Fig. 7b. Average of V_d shown in Fig. 7a, computed and plotted against target depth. A threshold voltage V_T can be set close to *Vos* above which indicates the presence of the metal.

V. Modified Sensor

The differential sensing scheme presented in sec. III had a sensing pair and a dummy pair, which were spatially separated. If these were combined into a single unit with a single primary and, secondary sensing and dummy windings, the number of leads would reduce and hence it would become less complex and more reliable [11]. Such a unit is shown in Fig. 8 below with the primary being excited from a DC source and the output of the sensing and dummy windings being fed to a differential amplifier to track the target.

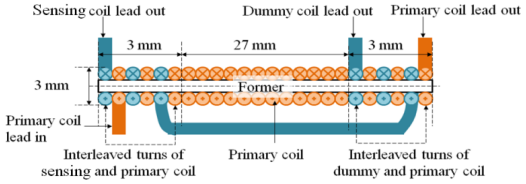

Fig. 8. Modified sensor.

The dimensions of the modified sensor are as indicated in Fig. 8. Here, since the turns of the sensing and the dummy coil were wound interleaved with the primary coil, the overall diameter of the sensor was only 3.6 mm, while it was 5.8 mm for the previous version. The primary coil had 86 turns while both the secondary coils had 6 turns each. The measured inductance and resistance of the primary coil are 2.62 µH and 340 mΩ respectively; while for the secondaries, these are 106 nH and 100 mΩ respectively.

The performance of the modified sensor for cylindrical targets of different type and cross sectional area, along its axis is listed in Table I below.

TABLE I On –Axis Measurement Range of Modified Sensor

Sr. No	Target	ID (mm)	OD (mm)	Cross Sectional area (mm^2)	Height (mm)	Detection depth (mm)
1	steel	2.5	6	23.35	10	≥ 11
2	steel	2.5	6	23.35	5	≥ 11
3	Copper (*Cu*)	2	10	75.36	5	≤ 10
4	Aluminium	2.5	5	14.72	6.5	≥ 5
5	*Cu* washer	2.5	6	23.35	0.5	≥ 5
6	Brass nut	2	4	9.42	2	≥ 3

In Table I, it can be observed that, the detection depth of the sensor has decreased, due to the reduction in diameter and number of turns of the sensing coil. It is more sensitive to inductive targets than conductive ones [7]. But, among targets of the same type, the one exposing greater cross sectional area along the sensor axis has greater detection range. This also implies that, a larger target produces a higher output than a smaller one for the same depth. This will be an issue if the objective is to measure the distance between sensor and target. So an alternative solution is to help the doctor by providing feedback whether he is approaching the target or deviating from it, while probing with the sensor in a particular direction. Considering this in view, an off-axis test was also done using the modified sensor with the setup shown in Fig. 9

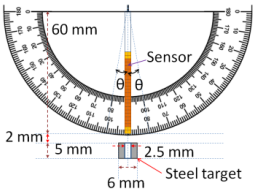

Fig. 9. Test setup for off-axis measurements and sliced view of the target.

In the test setup, the sensor was suspended from a pivot, on which it moved freely. Its angular displacements were measured using a protractor placed behind. A steel target of size shown above was placed linearly at a depth of 2 mm beneath it. The above position indicates 0 degree displacement of the sensor. Outputs of the sensor V_m for angular displacements up to ±10 degree were recorded. V_m is the difference of V_d and offset voltage V_{OS} of the sensor. The averages of V_m for various angular displacements are listed in Table II.

TABLE II Time Average of V_m for Various Angular Displacements

Angle (degrees)	-10°	-5°	0°	+5°	+10°
Minimim distance from sensor to target (mm)	8	3.5	2.0	3.5	8
V_m average (mV)	0.7	1.5	5.8	2.0	0.4

In Table II, it can be seen that the maximum output is at the vertical position and the output drops almost by the same manner to the left and right of the vertical position. This can be envisaged as, when the sensor is approaching the target, its output increases and when it is moving away, the output decreases. If this can be provided to the surgeon as an audio signal, he will hear a change in audio amplitude when he moves the sensor head towards the target. The audio amplitude will change in the opposite manner, if he has surpassed the target. Table II also highlights the effect of orientation of the target. When the sensor moves (angular) with respect to the target, the target orientation with respect to the sensor also changes accordingly. So here, the maximum detection range is only 8 mm, where as the linear detection range for the same target, for the same pulse excitation was 11 mm.

VI. Effect of Body Tissues on Sensor Performance

In sec. IV and V, the tests were performed in air. However, inside a human body, it will encounter body tissues, bones and other fluids. To test the modified sensor for such conditions, a phantom constituting 3 gm of KCl in 500 gm of de-ionized water [12] was prepared to emulate the tissue conductivity [13] at 10 µs excitation pulse fall time. The setup is as shown

in Fig. 10. There was a transparent tub to immerse the target as well as the sensing end of the sensor, in the phantom.

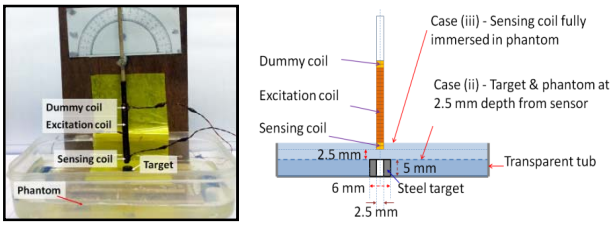

Fig. 10. Test setup - Target and phantom at 2.5 mm depth from sensor.

On-axis readings were recorded for target depths (T_d) of 2.5 mm and 6 mm from the sensor. For each of these depths, measurements were taken for (i) no phantom, (ii) phantom at a depth of 2.5 mm from the sensing coil and (iii) the sensing coil completely immersed in the phantom. The V_{OS} of the sensor was also measured. These are shown in Fig. 11 below.

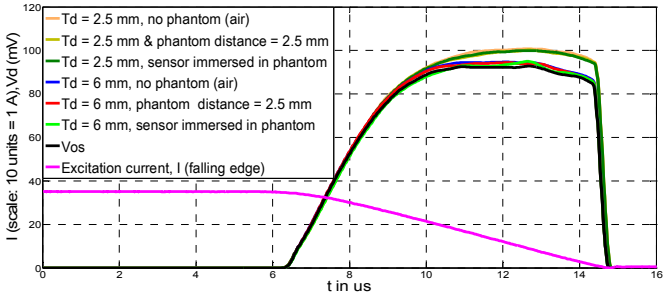

Fig. 11. Output of the sensor V_d for 2.5 mm and 6 mm depths of steel target.

In Fig. 11, when T_d is close, its outputs for different levels of the phantom are distinguishable from V_{OS}. But when T_d is large, the output voltages are in the range of the V_{OS} itself. Hence, to study the effect of the phantom, the voltage V_m was found for 6 mm depth of the target, for no phantom and different levels of the phantom. This is as shown in Fig. 12.

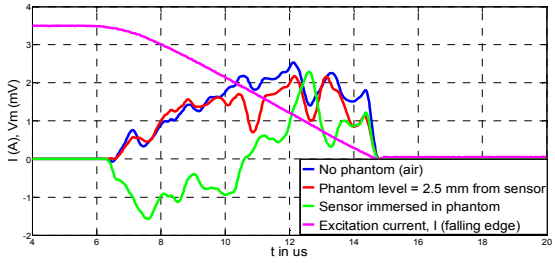

Fig. 12. V_m for 6 mm depth of target, for different levels of the phantom.

It can be seen in Fig. 12 that V_m decreases with increase in the level of the phantom. This is due to the fact that, the phantom provides a conductive environment around the sensor and becomes a resistive load, like the target. Hence, it can be interpreted that the tissue conductivity may reduce the output of the sensor, thereby decreasing the detection range by a small amount.

VII. Conclusion

A new inductive proximity sensor to help the doctor to trace metal shrapnel during the surgery is presented in this paper. Since the sensor has a size constraint when compared to conventional metal detectors, a differential sensing scheme is proposed to obtain accurate output. As a result, the prototype IPS developed can identify metal targets at depths much greater than its diameter. But, since this scheme has separate primaries which are spatially separated, the multiple leads present can affect the measurements. So a compact, modified version of the sensor was developed and tested for on-axis and off-axis measurements. The modified sensor seemed to be more versatile than the previous version during the tests, but its detection range was compromised due to the reduction in diameter and number of turns of the sensing coil. The performance results clearly indicate that the new IPS can contribute to the development of an online shrapnel detection tool. The shifts observed in the sensor output while it moves towards and away from the target, will form the basis of detection. This phenomenon will continue even when the sensor is inside the victim's body and therefore can be used to guide the surgeon using audio signals. Thus, the surgeon will get information about the position of shrapnel in relation to the sensor on an online basis and the surgery will become much more effective than using conventional means.

References

[1] S. Jacob, T. Sella, D. Shaham, S.C. Shapira, A. Rivkind, A.I. Bloom, and E. Libson, "Facing the new threats of terrorism: Radiologists' perspectives based on experience in Israel," *in Proc. Radiology*, Oct. 2005, vol. 237, pp. 28–36.

[2] M.K. Jameii, and M.A. Nekoui, "Improving the performance of the PI systems through the use of neural network," *in Proc. International Conference on Computer Engineering and Applications (ICCEA)*, Mar. 2010, vol. 1, pp. 561–566.

[3] J. Trevelyan, "Target depth estimation for a metal detector in the frequency domain," *in Proc. International conference on detection of abandoned land mines*, Oct. 1998, no. 458, pp. 218–221.

[4] C. Xin, C. Kim, M. Pramanik, and L.V. Wang, "Photo-acoustic tomography of foreign bodies in soft biological tissue," *Biomedical Optics J.*, vol. 16, no. 4, pp. 046017-1 - 046017-4, Apr. 2011

[5] Search Coils Tech Sheet. *Search Coil Basics,* [Online] Available: http://www.garrett.com

[6] R. Medek, J. Nicolics, and D. Schrottmayer, "High sensitive pulse inductive eddy current measurement for mine detection systems," *in Proc. International Spring Seminar on Electronics technology (ISSE),* May. 2001, pp. 207–211

[7] S. Yamazaki, and H. Nakane, "Basic analysis of a metal detector," *IEEE Trans. Instrum. Meas.*, vol. 51, pp. 810-814, Aug. 2002.

[8] A. Rerkratn, W. Petchmaneelumka, J. Kongkauroptham, K. Kraisoda, and A. Kaewpoonsuk, "Pulse induction metal detector using sample and hold method," *in Proc. International Conference on Control, Automation and Systems (ICCAS),* Oct. 2011, pp. 45–48.

[9] *Axial field of a finite, straight, thin shell solenoid*. [Online] Available: http://www.netdenizen.com/emagnet/solenoids/thinsolenoid.htm

[10] Minelab Technology. *Metal Detector Basics and Theory,* [Online] Available: http://www.minelab.com

[11] M. R. Nabavi, and S. N. Nihtianov, "Design Strategies for Eddy-Current Displacement Sensor Systems: Review and Recommendations," *IEEE Sensors J.*, vol. 12, no. 12, pp. 3346-3355, Dec. 2012.

[12] J.B. Jarvis, R. Kaiser, and M.D. Janezic, "Phantom Materials Used To Model Detection Of Concealed Weapons And Effects On Implant Devices In Metal Detectors", *in Proc. International Union of Radio Science (URSI) General Assembly*, Maastricht, Aug. 2002.

[13] Gabriel, S. Gabriely, and E. Corthout, "The Dielectric Properties of Biological Tissues: I. Literature Survey," *Phys. Med. Biol.*, vol. 41, no. 11, pp. 2231-2249, Nov. 1996.